JOURNAL OF PROPULSION AND POWER
Vol. 19, No. 4, July–August 2003

Flow Separation Inside a Supersonic Nozzle Exhausting into a Subsonic Compressible Crossflow

S. J. Beresh,* J. F. Henfling,† and R. J. Erven‡
Sandia National Laboratories, Albuquerque, New Mexico 87185

Surface pressure data have been acquired along the nozzle wall and surrounding the exit plane for an axisymmetric supersonic jet exhausting transversely from a flat plate into a subsonic compressible crossflow. These measurements have shown that the backpressure is sufficient to instigate nozzle flow separation under flowfield conditions that may be found in flight. The separation line has been found to be axially asymmetric, which results from the angular variation in the backpressure on the nozzle generated by the jet's interaction with the freestream. As either the jet-to-freestream momentum ratio or the crossflow freestream Mach number is independently reduced, the size of the separated flow region becomes larger because the backpressure on the nozzle is increased relative to the jet stagnation pressure. Schlieren imaging is consistent with these observations and provides further elucidation of the resulting jet shock wave structure. Comparison of the data to correlations derived from freejet separation data is possible by employment of these predictions in a piecewise fashion around the perimeter of the nozzle.

Nomenclature

J	=	jet-to-freestream dynamic pressure ratio, $(\gamma p_e M_e^2)/(\gamma p_w M_\infty^2)$
ℓ	=	nozzle axial position measured from throat
ℓ_{sep}	=	nozzle flow separation point
ℓ_0	=	nozzle expansion length
M_e	=	nominal jet exit Mach number
M_∞	=	freestream Mach number
P_0	=	freestream stagnation pressure
P_{0j}	=	jet stagnation pressure
p	=	pressure
p_b	=	backpressure on the jet
p_e	=	nominal perfectly expanded jet exit pressure
p_n	=	nozzle wall pressure
p_s	=	separation pressure inside the jet nozzle
p_w	=	freestream static wall pressure, measured upstream of the jet interaction
T_0	=	freestream stagnation temperature
T_{0j}	=	jet stagnation temperature
γ	=	specific heat ratio

Introduction

IF the backpressure placed on a supersonic nozzle is sufficiently large compared to the jet exit pressure, shock-induced separation will occur within the nozzle itself. When a jet is exhausted into a crossflow, the backpressure will vary around the exit orifice of the jet due to the pressure rise induced by stagnation at the leading edge of the jet and the decrease in pressure in its wake. If nozzle flow separation is present, this varying backpressure could create a similar azimuthal variation in the separation line; hence, the exiting flow may be strongly nonuniform despite the axisymmetric geometry of the nozzle.

Such axially asymmetric nozzle flow separation may have significant performance implications for vehicles employing jets for roll or attitude control at altitudes where the backpressure is sufficiently large. Although symmetric separation often increases the thrust of a nozzle by essentially redefining its geometry to reduce the overexpansion and improve the thrust efficiency,[1] it is conceivable that nonuniform separation will redirect the mean thrust vector produced by the nozzle. This would be consistent with the side loads that have been observed when separation is nonuniform in an axisymmetric nozzle during startup or shutdown transients.[1] Furthermore, the counter-rotating vortex pair that dominates the far field of the jet interaction may be altered. Given that the development of this vortex pair has been shown to originate from the nozzle itself,[2–5] a separated nozzle flow may influence the global behavior of the jet-in-crossflow flowfield and any interactions with downstream control surfaces. In fact, Kelso et al.[3] have shown in an incompressible flowfield that the development of the vortex pair was influenced by separation in the pipe from which their jet emanated.

Although studies of supersonic nozzle flow separation in jet-in-crossflow interactions appear absent from the open literature (although some researchers have examined the similar issue for incompressible flows[3,6]), numerous studies have examined nozzle separation in freejet configurations.[7–22] Such investigations are not directly applicable to a jet in crossflow because they do not provide for asymmetries in the backpressure. However, they potentially could be related to a nozzle exhausting into a crossflow if they are strictly applied only to a radial slice of the nozzle and repeatedly employed to build a representation of the separated flowfield in a piecewise fashion. On the other hand, three-dimensional influences may alter the flowfield sufficiently that the axisymmetric freejet studies are no longer applicable.

The present study aims to explore the flow separation inside a supersonic nozzle when it exhausts into a subsonic compressible crossflow. The primary measurements are mean surface pressures along the nozzle wall to locate the presence of separation and on the flat plate to ascertain the backpressure. These data are supported by schlieren images to reveal the resulting shock structure at the exit of the jet. Comparisons are made with correlations to freejet data that can be found in the open literature to determine the utility of such predictions in the analysis of nozzle performance when an interaction with a crossflow occurs.

Presented as Paper 2002-1067 at the AIAA 40th Aerospace Sciences Meeting and Exhibit, Reno, NV, 14–17 January 2002; received 11 July 2002; revision received 19 March 2003; accepted for publication 4 April 2003.

*Senior Member of the Technical Staff, Engineering Sciences Center, P.O. Box 5800, Mailstop 0834; sjberes@sandia.gov. Member AIAA.
†Distinguished Technologist, Engineering Sciences Center, P.O. Box 5800, Mailstop 0834.
‡Senior Technologist, Engineering Sciences Center, P.O. Box 5800, Mailstop 0834.

Experimental Apparatus

Trisonic Wind Tunnel

All experiments were performed in Sandia National Laboratories' Trisonic Wind Tunnel (TWT). The TWT is a blowdown-to-atmosphere facility with interchangeable test sections, each using air as the test gas. One is a transonic nozzle permitting a continuously variable Mach number from 0.5 to 1.3. The 305×305 mm^2 (12×12 in.^{2}) rectangular test section traditionally has been fitted with porous walls and is enclosed in a pressurized plenum to contain the flow that passes through them.

A solid-wall transonic test section was constructed to meet the needs of jet-in-crossflow experimentation. The porous walls have been replaced with solid walls both to supply a flat plate from which the jet will issue and to provide computationally tractable boundary conditions for comparison of experimental data and numerical simulations. Use of a wall-mounted jet was deemed superior to a sting-mounted flat plate to avoid such uncertainties as plate deflection and flow interference from the jet supply apparatus beneath the plate. The use of a solid-wall test section limits the Mach number range of the flowfield, but this was considered an acceptable compromise.

Supersonic Jet Hardware

Multiple conical nozzles have been fabricated. The three nozzles used herein have a design Mach number of 3.73 with an expansion half-angle of 15-deg and an exit diameter of 12.7 mm (0.500 in.), differing only in their instrumentation. One nozzle is instrumented with pressure taps on the flat plate from which the jet emanates to measure surface pressures beneath the jet-in-crossflow interaction, and a second nozzle is instrumented within the nozzle itself to allow an examination of internal flow separation. The remaining nozzle is uninstrumented. Any of the interchangeable nozzles may be connected to a settling chamber located behind either the top wall of the test section or one of the side walls. The settling chamber is supplied by a manifold of six nitrogen bottles to a maximum of 14 MPa (2000 psi) and is instrumented with a transducer and a thermocouple to provide stagnation pressure and temperature measurements.

Potential mounting positions for the jet are limited by the wind-tunnel support structure behind the test-section walls, so that two different locations have been employed to provide either alignment with the tunnel's windows or easy instrumentation access (Fig. 1). For the schlieren images, the jet was mounted on the top wall, where it is properly aligned with the windows. Constricted access precluded the utilization of this configuration for routine use of pressure instrumentation; therefore, for these measurements, the jet apparatus was mounted in a side-wall position by securing it in a window blank. The primary difference between these two arrangements is that the wind-tunnel wall boundary-layer thickness is about 10% less for the top wall as compared to the side wall, but the resulting impact on the jet-in-crossflow interaction has been shown to be insignificant.[23]

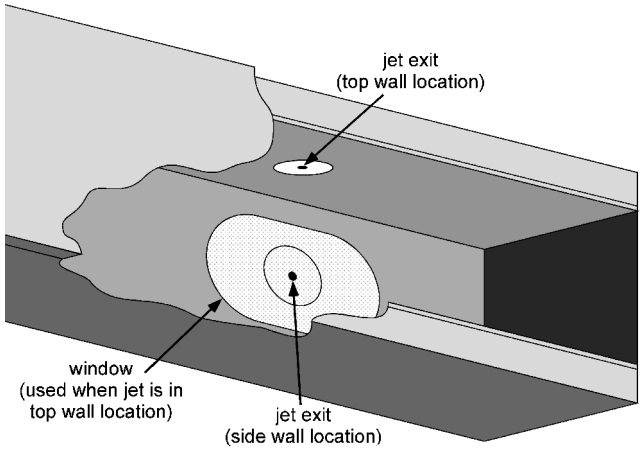

Fig. 1 Two jet nozzle mounting locations in the wind tunnel; flow is from left to right (not to scale).

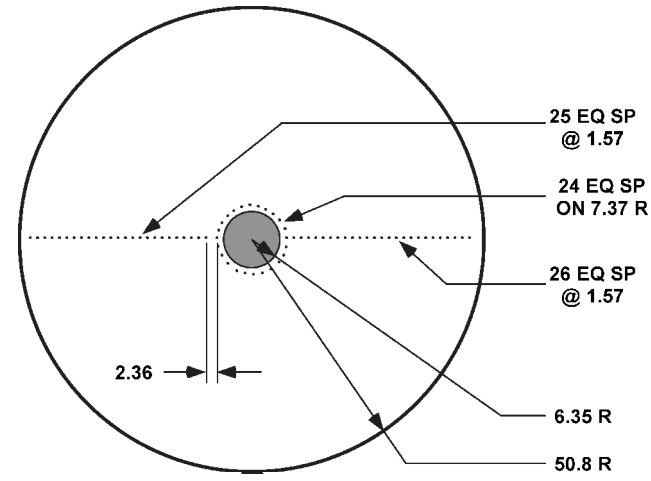

a)

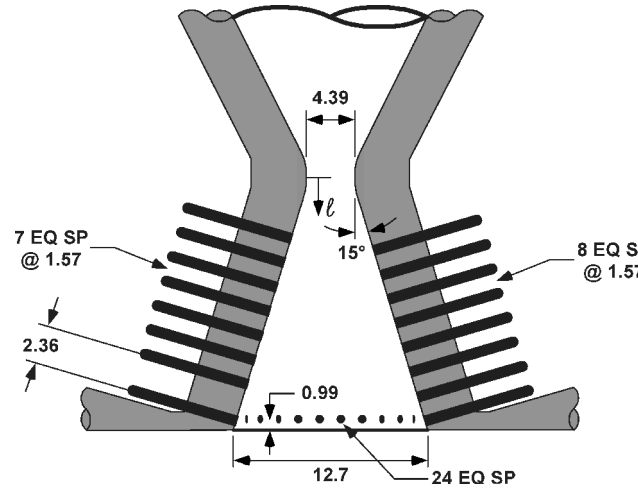

b)

Fig. 2 Pressure tap locations for each of the two instrumented nozzles: a) instrumented flat plate and b) instrumented within the nozzle; all dimensions are in millimeters and all taps are 0.51 mm in diameter.

The nozzle pressure instrumentation is shown in Fig. 2. Figure 2a shows the nozzle that is instrumented on the flat plate from which it exhausts. A ring of 24 taps surrounds the exit plane of the nozzle and two radial rows of taps 180 deg apart extend outward for a distance of approximately four jet diameters from the nozzle exit. The diameter of all pressure taps is 0.51 mm (0.020 in.) and tap spacing is typically 1.57 mm (0.062 in.).

The second instrumented nozzle has pressure taps only within the nozzle itself (Fig. 2b). A circumferential ring of taps is placed near the exit plane of the nozzle, and two rows of taps begin near the exit and extend about two-thirds of the way toward the nozzle throat. These two rows are offset with respect to one another by one-half of a pressure tap spacing. Thus, if the nozzle is rotated 180 deg and reinstalled, the pressure taps from one row fill the gaps between tap locations in the preceding orientation, effectively doubling the spatial resolution of the mean measurements. The nozzle is designed such that it can be installed into the test section at any chosen angle. Repositioning the taps between wind-tunnel runs produces a detailed mapping of the mean surface pressure field inside the nozzle. A dial on the nozzle and an indicator mounted on the test-section wall combine to permit accurate measurements of the radial position of the pressure taps. As in the first nozzle, the tap diameter is 0.51 mm and the tap spacing is typically 1.57 mm.

Instrumentation

Pressure measurements were made using a Pressure Systems, Inc., Model 8400 electronically scanned pressure system.

Measurements from each pressure port were acquired simultaneous with measurements of the stagnation pressure and temperature of both the wind tunnel and the jet settling chamber. The wind-tunnel static pressure p_w is found from wall measurements located 27 jet diameters upstream of the center of the jet exit, and the freestream Mach number M_∞ is determined assuming an isentropic expansion by the use of the ratio of p_w and P_0. For each wind-tunnel run, 400 individual data points from each pressure port were acquired at a rate of 100 Hz, then averaged to provide the mean data presented here.

The accuracy of the pressure measurements may be affected by the small size of the nozzle itself with respect to the pressure tap diameter. If the diameter of the pressure tap is a significant fraction of the boundary-layer thickness of the flow passing over it, some measurement bias may result.[24–30] When the analysis of Ducruet[30] is adapted to the present flowfield, it is clear that no significant bias will occur for measurements made on the flat plate where the wind-tunnel wall boundary layer is much larger than the pressure tap diameter. In contrast, the boundary-layer thickness within the nozzle is substantially smaller with respect to the pressure tap diameter, which may lead to appreciable measurement biases. Additional effects due to large velocity gradients and wall curvature tend to aggravate the potential for error. Ducruet's[30] work can be extrapolated to the present case by computing the largest velocity gradients found in the nozzle expansion (excluding those due to proximity to a shock) and the largest nozzle wall curvature, then extracting the corresponding worst-case bias found over the range of subsonic compressible Mach numbers examined by Ducruet. Although this estimate does not account for supersonic Mach number effects, Flack's[28] study suggests that they will not alter the magnitude of the bias. From this analysis, it appears that the wall curvature and velocity gradient effects only contribute substantially near the nozzle throat. The remaining bias due to the tap diameter is present throughout and may be no worse than +0.01 in terms of p_n/P_{0j}. However, because the primary purpose of the present study is to ascertain the presence of flow separation, these biases should not create a difficulty because separation is characterized by a distinct pressure rise, regardless of whatever biases may be superimposed on it.

Just as the large size of the pressure taps with respect to the nozzle boundary-layer thickness may create an effect on the measurements, the presence of the pressure taps themselves may create an effect on the nozzle flowfield. The Moulden et al.[27] study suggests that, in the present geometry, the nozzle flow may experience a perturbation generated by the pressure taps. For this reason, a nozzle was fabricated without any pressure taps to generate an unperturbed flowfield, which was used for schlieren imaging.

For the schlieren imaging, the flow was illuminated with a 1.4-μs duration (full-width half-maximum) xenon flashlamp and imaged with a 10-bit 1024 × 1024 pixel charge-coupled device camera (Pulnix TM-1010) captured by a digital frame grabber (National Instruments IMAQ 1424). The knife edge was oriented parallel to the nozzle exit plane.

Results and Discussion

Experimental Conditions

The testing conditions have been selected to approximate those found on transonic flight vehicles that employ supersonic jets for attitude or roll control. The primary freestream Mach number was $M_\infty = 0.8$, with a wind-tunnel stagnation pressure $P_0 = 154$ kPa (22.4 psia), which yields a test-section static pressure $p_w = 101$ kPa (14.7 psia). The wind-tunnel Reynolds number at these conditions is 20×10^6 m^{-1} (6×10^6 ft^{-1}). The nominal stagnation pressure for the Mach 3.73 jet was $P_{0j} = 4.96$ MPa (720 psia), which provided a perfectly expanded jet exit pressure of $p_e = 47.1$ kPa (6.84 psia). These conditions combine to produce a nominal $J = 10.2$. Six additional cases also were employed to span a range of J values while a constant $M_\infty = 0.8$ was maintained, or to span a range of subsonic values of M_∞ while a constant $J = 10.2$ was maintained. The choice of M_∞ and J must keep within the subsonic restrictions imposed by the tunnel blockage issues inevitable with the solid-wall transonic test section.[31]

Table 1 Experimental conditions for the jet and wind tunnel

Case	M_∞	P_0, kPa	P_w, kPa	P_{0j}, MPa	P_e, kPa	J
1	0.8	154	101	4.96	47.1	10.2
2	0.8	154	101	4.14	39.3	8.4
3	0.8	154	101	2.76	26.2	5.6
4	0.8	154	101	1.38	13.1	2.8
5	0.7	141	101	3.79	36.0	10.2
6	0.6	130	101	2.83	26.9	10.2
7	0.5	121	101	1.93	18.3	10.2

The nominal conditions for the seven test cases are shown in Table 1. The gas supply for the jet was unheated, and so the jet stagnation temperature T_{0j} was found to vary from 288 to 300 K (518–540°R) depending on the laboratory ambient conditions. The wind-tunnel air supply is heated in the storage tanks, but not temperature-controlled subsequent to this; therefore, the freestream stagnation temperature T_0 is also subject to variation and fluctuated from 308 to 325 K (554–585°R). These variations were incorporated into the calculation of the precision uncertainty, which was found to be small (discussed hereafter).

At the location on the wind-tunnel side wall from which the jet exhausts, the 99% velocity boundary-layer thickness has been measured as 12.7 ± 0.5 mm (0.50 ± 0.02 in.) with a pitot probe survey.

The Reynolds number of the nozzle flow based on the nozzle exit conditions and nozzle length is estimated as 7×10^6 for the nominal conditions. This is expected to be turbulent,[16] but may retain some degree of transitional character.

Surface Pressure Measurements

Surface pressure measurements have been conducted on both the flat plate (that is, the wind-tunnel side wall) and on the nozzle's interior wall. Extensive results for the flat-plate were reported in Refs. 23 and 31. The primary utility of the flat-plate measurements in the present study is to provide data concerning the variation of the backpressure around the nozzle's exit orifice (Fig. 3). Figure 3a shows the data from experimental conditions where M_∞ remained constant and P_{0j} (and, hence, J) was varied. Figure 3b presents data where J remained constant and M_∞ varied. As anticipated, the pressure rises substantially at the upstream edge of the jet (0 deg) where the crossflow stagnates against it; it is at this location that the axisymmetric nozzle will be most prone to internal separation. Analogously, the lowest backpressures are found in the jet's wake (near ±180 deg), and separation will be least likely there. Although scaling the pressure to p_w shows a decrease in the backpressure at the upstream edge with diminishing J or M_∞, the backpressure actually increases relative to P_{0j}, which is decreased to achieve the desired value of J, as shown in Table 1.

The internal nozzle wall pressures p_n along a line on the upstream edge of the nozzle are shown in Fig. 4. This portion of the nozzle flow will exhaust onto the wind-tunnel centerline and will experience the maximum backpressure as shown at 0 deg in Fig. 3. As in Fig. 3, Figs. 4a and 4b independently display the effects of varying P_{0j} and M_∞. Pressure data were combined from two different wind-tunnel runs, one of which rotated the nozzle by 180 deg to interleave the pressure taps for greater spatial resolution. This accounts for the waviness observed in some of the pressure traces, which resulted from a slightly nonuniform expansion through the nozzle as opposed to run-to-run variations or the influence of the crossflow (possibly due to machining tolerances or other imperfections). When the nozzle was rotated 180 deg, this nonuniformity rotated 180 deg as well, so that each of the two lines of taps measured slightly different pressure distributions, regardless of rotational position. Further details are discussed in Ref. 23. Additional wind-tunnel runs demonstrated that the repeatability of the data, including the nonuniform interleaving, is excellent. The run-to-run precision uncertainty was found to be approximately the thickness of the curves in Fig. 4.

Despite the small nonuniformity due to the pressure tap interleaving, Fig. 4 shows that flow separation is clearly indicated by

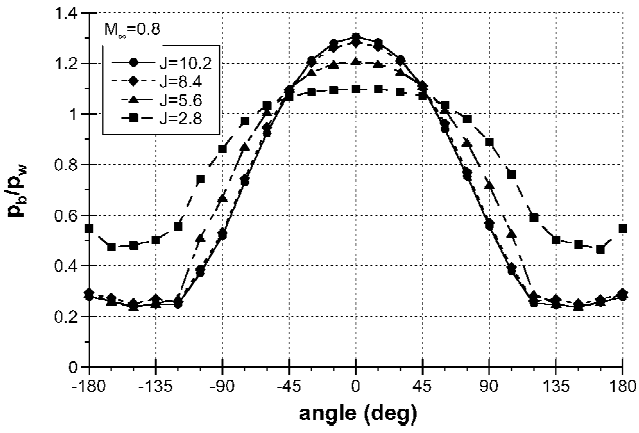

a)

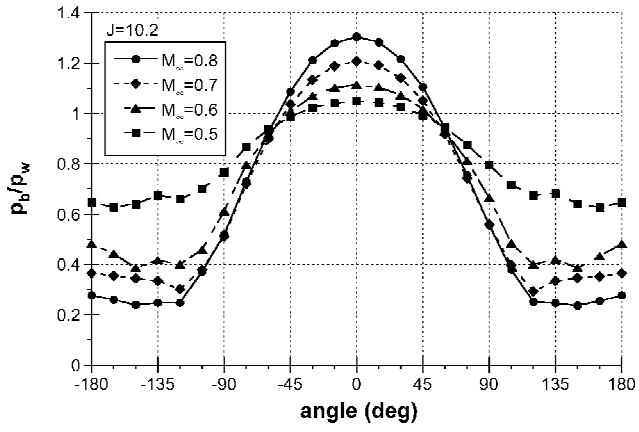

b)

Fig. 3 Mean surface pressures on the flat plate around an annulus surrounding the jet exit, displaying the variation in the backpressure induced by the jet-in-crossflow interaction: a) J is varied and M_∞ remains constant and b) M_∞ is varied and J remains constant; the upstream edge of the jet is located at 0 deg.

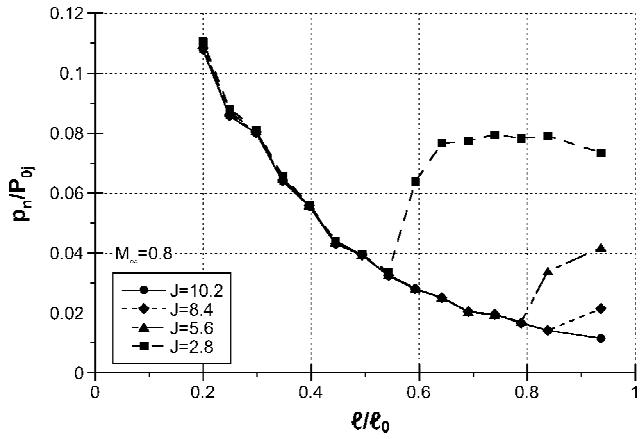

a)

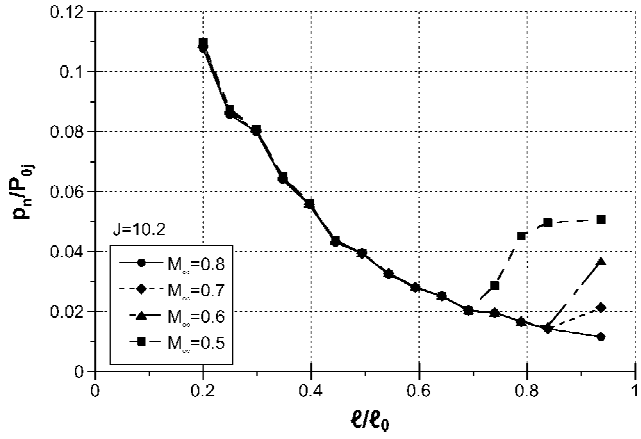

b)

Fig. 4 Mean nozzle internal wall pressures along a line on the nozzle's upstream edge: a) J is varied and M_∞ remains constant and b) M_∞ is varied and J remains constant.

a distinct rise in surface pressure as the nozzle exit is approached. The precision of determining the separation point is limited by the spatial resolution offered by the pressure taps in such a small nozzle. Figure 4 demonstrates that, despite this difficulty and any bias in the pressure measurements due to the relatively large diameter of the taps, it is possible to identify flow separation within the nozzle.

It is evident in Fig. 4 that no separation occurs at the nominal flow conditions of $J = 10.2$ and $M_\infty = 0.8$, despite the increase in backpressure above the freestream static pressure resulting from the jet-in-crossflow interaction. However, as either J or M_∞ is reduced, separation is observed, where smaller values of J or M_∞ produce a larger separation region and a greater pressure rise. Decreasing J while M_∞ remains constant is analogous to raising the backpressure for a fixed P_{0j}. Reducing M_∞ from its nominal value of 0.8 induces separation, despite the constant $J = 10.2$, because the smaller value of M_∞ demands a proportionally larger value of p_w/p_e to maintain the value of J. Hence, the backpressure increases sufficiently to induce separation. The parameter most strongly controlling the location of the separation point is the pressure ratio P_{0j}/p_b, where p_b is the local backpressure, but this value varies around the nozzle perimeter due to the jet-in-crossflow interaction. The use of J and M_∞ to describe the flowfield is convenient because it determines the p_b distribution.

To determine the variation of the separation point around the perimeter of the nozzle, the azimuthal angle of the pressure taps was adjusted from one wind-tunnel run to the next. This procedure produced pressure traces comparable to those seen in Fig. 4, but because of their similarity to those already shown, they are omitted here, but may be found in Ref. 23. At each of these angular positions, the separation point was determined by the assumption that separation occurs at the point midway between those pressure taps where the pressure was observed to rise above its unseparated value. These individually determined points were then assembled into a trace of the separation line as though the nozzle wall had been laid out flat. This is done in Fig. 5 for the six test cases at which separation was observed. The error bounds shown represent the limits of the spatial resolution due to the distance between adjacent pressure taps, which dominate other error sources such as the uncertainties in the measured pressure or the azimuthal nozzle orientation. The bias due to the pressure tap size is relatively constant near a particular tap and, thus, does not contribute appreciably to error in locating the separation point. For virtually all data points, the separation pressure was found to be strongly in excess of the precision uncertainty of the pressure measurement, which made the determination of the separation point quite dependable. Flowfield symmetry was invoked to reflect the data about the wind-tunnel centerline and, thus, trace the separation line around the entire nozzle perimeter. Symmetry was verified by experimentation.[23]

Also shown in Fig. 5 are the locations of the separation points as determined by four different predictive methods. Although these data correlations were developed from freejet experiments, they have been applied in the present case by examining the flowfield one radial slice at a time. At each angle about the nozzle perimeter, the backpressure was determined from the data shown in Fig. 3 and used in conjunction with P_{0j} to predict the separation point for that angle, as if the entire jet exhausted into an ambient at the equivalent pressure. (For engineering design applications where the backpressure distribution is not known, reasonable estimates may be derived from one or more of the studies referenced in Margason's survey paper[32] that correlate such pressure distributions to common similarity parameters, or from an empirical or numerical model such as

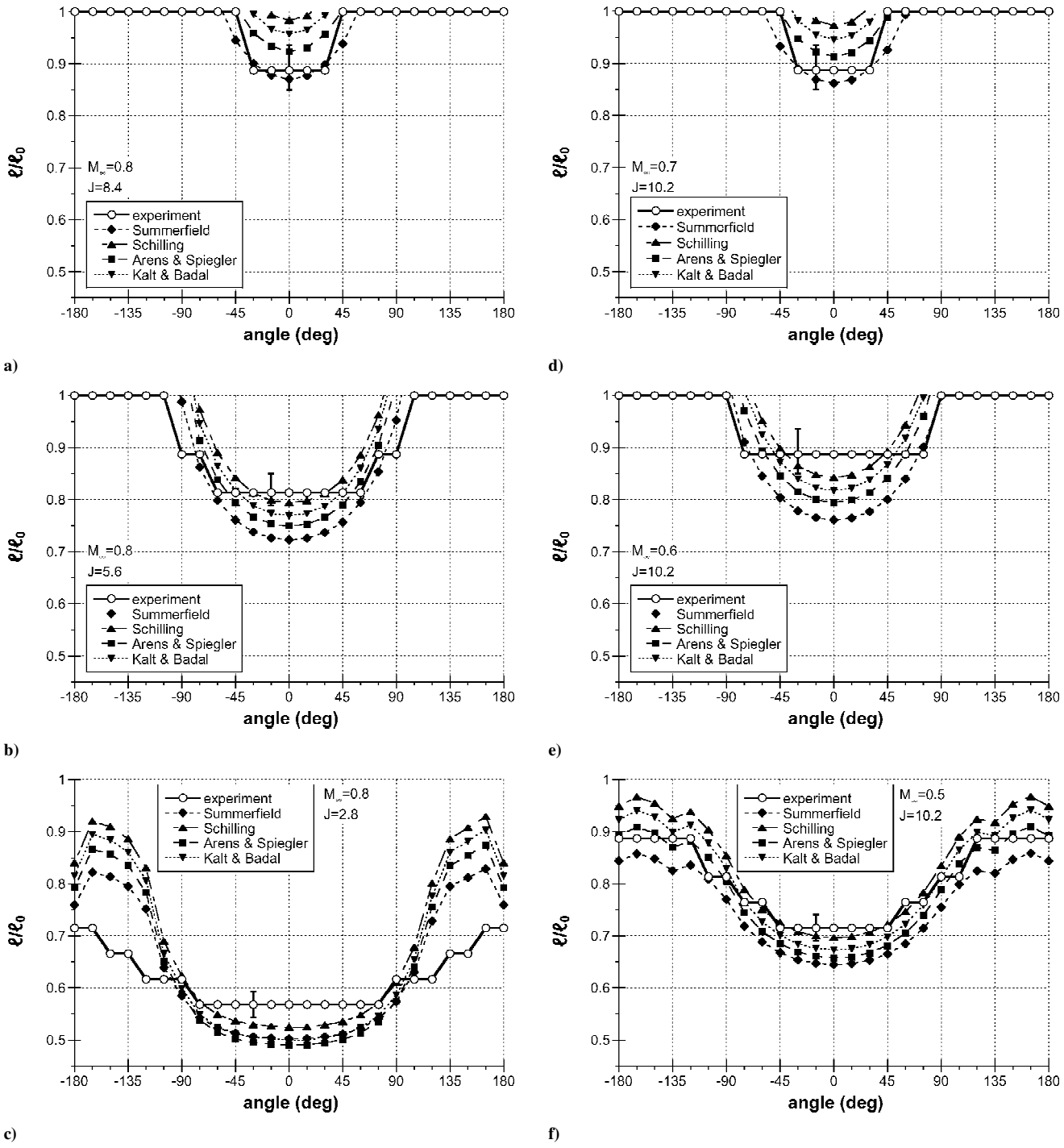

Fig. 5 Flow separation lines within the jet nozzle determined from mean surface pressure data and compared with separation lines from four predictive methods; flowfield conditions are given for figs. 5a–5f, each of which shows sample error bounds representing the spatial resolution of the experimental data.

those discussed by Cassel et al.[33]) Repeated calculations for each angle and unique backpressure built up a prediction of the separation line. If no predictive location is shown in Fig. 5, then the correlation indicates no separation.

The first prediction examined was the well-known the Summerfield criterion[8]

$$p_s = 0.4 p_b \tag{1}$$

which, although simplistic and limited in its accuracy,[13,16] is still sufficiently reliable to find general utility.[1,21] Another useful predictor is Schilling's correlation[10] to a large quantity of freejet separation data, given by

$$(p_b - p_s)/P_{0j} = 0.494(P_{0j}/p_b)^{-0.906} \tag{2}$$

Schilling also offers a correlation specifically to separation data from 15-deg half-angle conical nozzles, as in the present experiment, but the results are not appreciably different from those of the broadly applicable Eq. (2). Also examined in the present analysis is the semi-empirical approach of Arens and Spiegler[11] using the equations

$$\frac{p_b}{p_s} = \frac{[2.16 f(p)]^{3.5}}{[1 + 0.64 f(p)][1.993 f(p) - 0.167]^{2.5}} \tag{3a}$$

$$f(p) = \left(\frac{P_{0j}}{p_s}\right)^{(1/3.5)} - 1 \tag{3b}$$

which were derived from Eqs. (3) and (4) of Ref. 11 by setting $\gamma = 1.4$ and $u_s^*/u_s = 0.6$. The final correlation was that of Kalt

and Badal,[14]

$$p_s/p_b = \tfrac{2}{3}(P_{0j}/p_b)^{-0.2} \quad (4)$$

which is fit to a smaller quantity of data than Schilling's correlation.

All four correlations produce fairly similar predictions, none of which is obviously superior to the others. This is partly because the limited spatial resolution of the experimental data makes it difficult to evaluate small differences between the predictions, but it is also because different correlations appear to yield better results when the flowfield conditions are altered. The only case in which all four predictions misrepresent the data is Fig. 5c, where both the leading-edge separation of the nozzle is overpredicted and the lesser separation at the nozzle's trailing edge is underpredicted. The trends of the other five cases are reasonably predicted by all four correlations, with some differences between them. The Summerfield[8] criterion produces a reasonably good match for the limited separation regions of Figs. 5a and 5d, but overpredicts the degree of separation for the other cases. Schilling's correlation[10] produces precisely opposite behavior, where it underpredicts the separation zone for Figs. 5a and 5d, but does a respectable job in the other cases. Both the Arens and Spiegler[11] prediction and the Kalt and Badal[14] correlation consistently lie between the Summerfield and the Schilling correlations.

It is not clear why the correlations perform poorly for the completely (though non-uniformly) separated case of Fig. 5c, but produce better results for the similar case of Fig. 5f. A possible answer is that three-dimensional flow in the separated region induced by the variation in backpressure about the nozzle exit is responsible for altering the pressure downstream of the shock, which in turn adjusts its position within the nozzle to accommodate the new pressure ratio. Figure 3a shows that the backpressure difference from the leading edge of the nozzle to the minimum in the jet's wake for the case where $J = 2.8$ and $M_\infty = 0.8$ (Fig. 5c) is about $\Delta p_b/p_w = 0.63$, whereas Fig. 3b shows that, for $J = 10.2$ and $M_\infty = 0.5$ (Fig. 5f), $\Delta p_b/p_w = 0.42$. The larger pressure gradient for the former case may induce stronger circumferential flow than the latter case, which accounts for the greater deviation from the correlations seen in Fig. 5c. Similar three-dimensional flow would be expected for the four partially separated cases, but the smaller $\Delta p_b/p_w$ within their separated regions may not be sufficient to induce as distinct a result as in Fig. 5c. Furthermore, the shock position may be influenced by the inflow into the nozzle separation region of the separated flow on the flat plate (i.e., the horseshoe vortices wrapped around the jet immediately following its exit from the nozzle), whose nature may contribute to the greater deviation from the correlations observed in Fig. 5c as compared to Fig. 5f.

To assess the predictive capabilities of the correlations in a more quantitative manner, their deviation from the experimental data was determined. This was accomplished for each correlation and each experimental case by summing over all data points the distance between the predicted and measured separation location. If the prediction lay within the spatial resolution of the measurement, that is, the error bounds shown in Fig. 5, the deviation was considered to be zero. The results are presented in Table 2, where the values are given in terms of ℓ_{sep}/ℓ_0.

These results confirm the qualitative assessment of the correlations' performance. The Summerfield criterion has less error than the other three predictions for cases 2 and 5, where the separation zone is smallest, but the most error in the other cases (excepting case 4, where all correlations perform poorly and it probably is not meaningful to decide which is best). Schilling's correlation performs the best when the size of the separation zone is significant, but is more prone to inaccuracy when separation occurs nearer the nozzle exit. Such inaccuracy has been observed in other investigations as well,[11–13,16] possibly because the stagnated freestream flow that is circulated into the lip of the nozzle plays a greater role when the separation shock is nearby. Kalt and Badal's correlation tracks the performance of Schilling's correlation fairly closely. Arens and Spiegler's prediction is the most successful of the four correlations, behaving similarly to the Summerfield criterion when it performs best and similarly to Schilling's correlation when it is superior. However, the equations of Arens and Spiegler must be solved through an iterative process, whereas either Schilling's or Kalt and Badal's correlations may be more attractive due to their ease of use. Schilling's correlation has the added attraction of having been validated by comparison with a detailed analytical method.[19]

Table 2 Total deviation of the nozzle separation predictions from the experimental data, given in terms of ℓ_{sep}/ℓ_0, for each correlation and experimental case[a]

Researchers	Case 2, Fig. 5a	Case 3, Fig. 5b	Case 4, Fig. 5c	Case 5, Fig. 5d	Case 6, Fig. 5e	Case 7, Fig. 5f
Summerfield et al.[8]	0.12	0.69	1.75	0.14	0.85	1.25
Schilling[10]	0.52	0.51	2.40	0.50	0.47	0.78
Arens and Spiegler[11]	0.14	0.50	2.28	0.12	0.66	0.48
Kalt and Badal[14]	0.44	0.51	2.39	0.38	0.55	0.64

[a]These deviations were found by summing the distance between the predicted and measured separation location over all data points.

As noted earlier, the discrepancies between the predictions and the experimental data may be influenced by a degree of three dimensionality not present in the data to which the correlations were fit. Also note that the precise backpressure is not well known; the backpressure measurements on the flat plate were made a finite distance from the edge of the jet orifice and the actual backpressure at the jet may be somewhat different. In addition, Morrisette and Goldberg noted that laminar flow in a separated nozzle may deviate from typical data correlations.[16] Whereas the present nozzle flow is expected to have transitioned to turbulence, the nozzle Reynolds number is not strongly in excess of its critical value, especially at low P_{0j} conditions, and this may be a contributor to deviation from the correlations.

Schlieren Images

Although the utility of schlieren imaging is limited by its integrating nature and its inability to look inside the nozzle itself, it still provides insight into the behavior of the jet under separated conditions. Figures 6 and 7 show the schlieren images for all seven experimental cases. Figure 6 displays the effects of lowering J while maintaining $M_\infty = 0.8$, and Fig. 7 shows those for lowering M_∞ while $J = 10.2$. The case of $M_\infty = 0.8$ and $J = 10.2$ is common to both Figs. 6 and 7, but is given only in Fig. 6a. The images shown are averages of 20 instantaneous images.

The position of the oblique shock at the nozzle's leading edge (the left side of the images) can be seen to change in Fig. 6 as J is reduced and nozzle flow separation becomes more prominent. At $J = 8.4$, it has moved slightly toward the nozzle centerline, and at $J = 5.6$ its inward position is more discernable. By $J = 2.8$, this oblique shock exits the nozzle nearly at its centerline, and the trailing-edge oblique shock also has moved inward. These observations are consistent with the increase in the size of the separation region with diminishing J that was determined from the pressure measurements. The off-center position of the oblique shocks seen for $J = 2.8$ corresponds to the greater degree of separation at the leading edge of the nozzle as compared to its trailing edge, as was shown in Fig. 5c. A further observation reveals that as the oblique shocks move toward the nozzle centerline, the leading edge of the jet interface also moves inward. This presumably corresponds to the position of the shear layer generated at the point of separation inside the nozzle.

Similar trends are observed in Fig. 7 as M_∞ decreases while J remains constant. The leading-edge oblique shock moves toward the nozzle centerline for lower M_∞, and the associated shear layer also can be observed to move inward slightly at $M_\infty = 0.5$, as does the trailing-edge oblique shock. The position of the oblique shocks is not as close to the centerline in Fig. 7d as in Fig. 6d, which is consistent with the smaller, though fully separated, region seen in the pressure measurements in Fig. 5f as opposed to Fig. 5c. Figure 7 also indicates that, in contrast to Fig. 6, the jet penetration into the crossflow is roughly identical for all four cases. This supports the conventional notion that J is the most influential parameter governing jet penetration.[32,34–36]

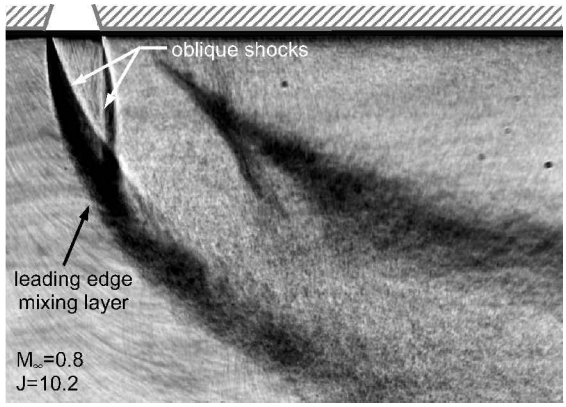

a)

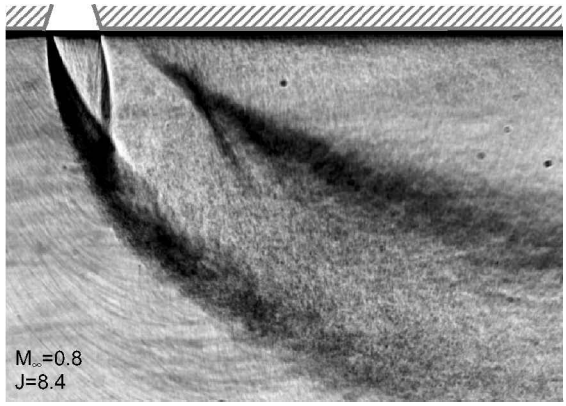

b)

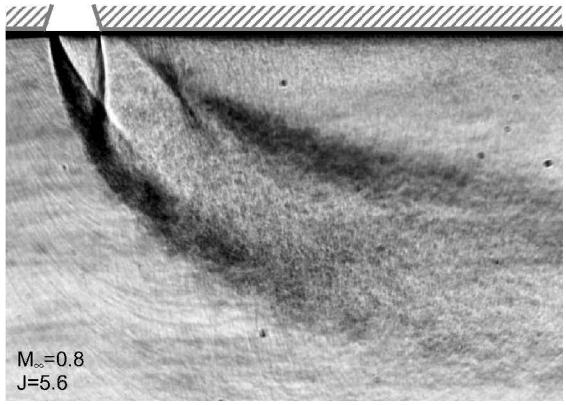

c)

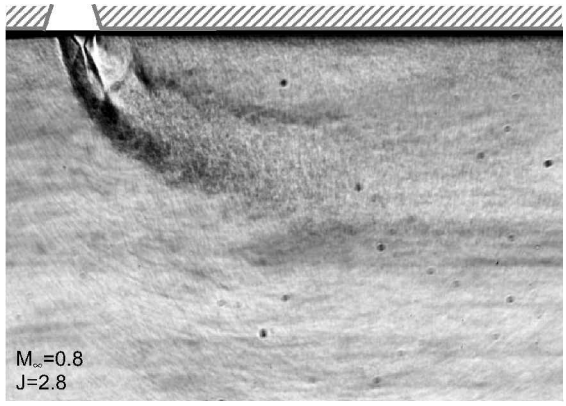

d)

Fig. 6 Schlieren images of the jet in crossflow, including the shock structure generated by nozzle flow separation, for a constant $M_\infty = 0.8$, while J is reduced; flowfield conditions are given in each case, and the freestream flow is from left to right.

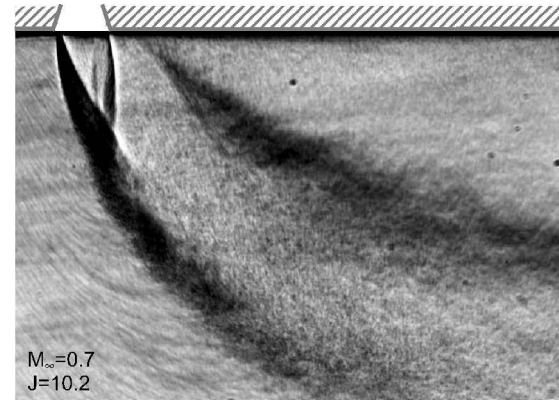

a)

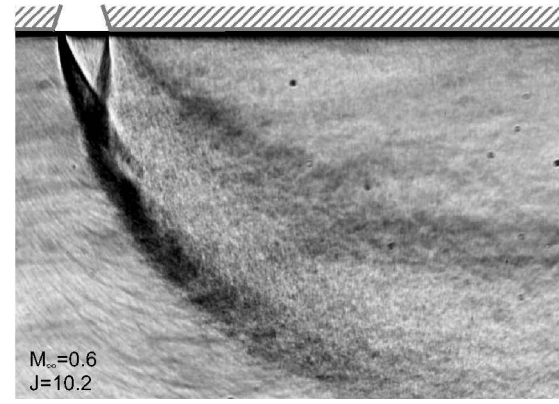

b)

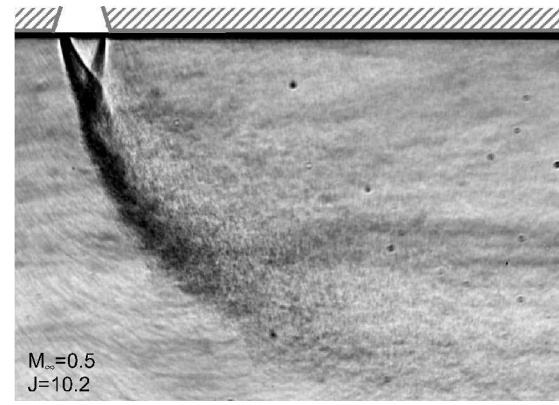

c)

Fig. 7 Schlieren images of the jet in crossflow, including the shock structure generated by nozzle flow separation, for a constant $J = 10.2$ while M_∞ is reduced; flowfield conditions are given in each case, and the freestream flow is from left to right.

Summary

Surface pressure data have been acquired on the nozzle wall and an annulus surrounding the exit plane for an axisymmetric supersonic jet exhausting transversely from a flat plate into a subsonic compressible crossflow. These measurements have shown that nozzle flow separation does occur under flowfield conditions that may be found on flight vehicles. Furthermore, the axially asymmetric nature of the separation has been identified, which results from the angular variation in the backpressure on the nozzle generated by the jet's interaction with the freestream. As either the jet-to-freestream momentum ratio J or the freestream Mach number M_∞ is reduced while the other is held constant, the size of the separated flow region becomes larger because the backpressure on the nozzle is increased relative to the jet stagnation pressure. Schlieren imaging is

consistent with these observations and provides further elucidation of the resulting jet shock wave structure.

The shape of the nozzle flow separation line has been determined for a variety of flow conditions and compared with the predictions from four different correlations to freejet separation data. Although these correlations were derived assuming a uniform backpressure, they have been used in the present study by their sequential application to radial slices of the nozzle and to building a trace of the separation line in a piecewise fashion. It has been shown that, in most cases, the correlations are in reasonable agreement with the data. Only when the nozzle is separated about its entire perimeter (but still possesses a nonuniform separation line) might the correlations yield unsatisfactory results. This may be a result of circumferential flow in the separated region induced by the angular variation in backpressure.

Acknowledgments

This work is supported by Sandia National Laboratories and the United States Department of Energy. Sandia is a multiprogram laboratory operated by Sandia Corporation, a Lockheed Martin Company, for the U.S. Department of Energy under Contract DE-AC04-94AL85000. The authors would like to thank the following Sandia National Laboratories staff members for their insightful advice and discussions: V. A. Amatucci, W. L. Oberkampf, J. L. Payne, C. W. Peterson, M. R. Prairie, C. J. Roy, W. H. Rutledge, and W. P. Wolfe.

References

[1]Sutton, G. P., *Rocket Propulsion Elements*, 6th ed., Wiley, New York, 1992, pp. 63–65.

[2]Sykes, R. I., Lewellen, W. S., and Parker, S. F., "On the Vorticity Dynamics of a Turbulent Jet in a Crossflow," *Journal of Fluid Mechanics*, Vol. 168, 1986, pp. 393–413.

[3]Kelso, R. M., Lim, T. T., and Perry, A. E., "An Experimental Study of Round Jets in Cross-Flow," *Journal of Fluid Mechanics*, Vol. 306, 1996, pp. 111–144.

[4]Haven, B. A., and Kurosaka, M., "Kidney and Anti-Kidney Vortices in Crossflow Jets," *Journal of Fluid Mechanics*, Vol. 352, 1997, pp. 27–64.

[5]Yuan, L. L., Street, R. L., and Ferziger, J. H., "Large-Eddy Simulations of a Round Jet in Crossflow," *Journal of Fluid Mechanics*, Vol. 379, 1999, pp. 71–104.

[6]Andreopoulos, J., "Measurements in a Jet-Pipe Flow Issuing Perpendicularly into a Cross Stream," *Journal of Fluids Engineering*, Vol. 104, Dec. 1982, pp. 493–499.

[7]Green, L., Jr., "Flow Separation in Rocket Nozzles," *ARS Journal*, Vol. 23, No. 1, Jan.–Feb. 1953, pp. 34–35.

[8]Summerfield, M., Foster, C. R., and Swan, W. C., "Flow Separation in Overexpanded Supersonic Exhaust Nozzles," *Jet Propulsion*, Vol. 24, No. 5, Sept.–Oct. 1954, pp. 319–321.

[9]Page, R. H., "Flow Separation in Nozzles," *Journal of the Aerospace Sciences*, Vol. 29, No. 1, Jan. 1962, pp. 110–111.

[10]Schilling, M., "Flow Separation in a Rocket Nozzle," M. S. Thesis, Graduate School of Arts and Sciences, Univ. of Buffalo, Buffalo, NY, June 1962.

[11]Arens, M., and Spiegler, E., "Shock-Induced Boundary-Layer Separation in Overexpanded Conical Exhaust Nozzles," *AIAA Journal*, Vol. 1, No. 3, 1963, pp. 578–581.

[12]Arens, M., "The Shock Position in Overexpanded Nozzles," *Journal of the Royal Aeronautical Society*, Vol. 67, No. 628, April 1963, pp. 268–269.

[13]Sunley, H. L. G., and Ferriman, V. N., "Jet Separation in Conical Nozzles," *Journal of the Royal Aeronautical Society*, Vol. 68, Dec. 1964, pp. 808–818.

[14]Kalt, S., and Badal, D. L., "Conical Rocket Nozzle Performance under Flow-Separated Conditions," *Journal of Spacecraft*, Vol. 2, No. 3, 1965, pp. 447–449.

[15]Miller, E. H., and Migdal, D., "Separation and Stability Studies of a Convergent–Divergent Nozzle," *Journal of Aircraft*, Vol. 7, No. 2, 1970, pp. 159–163.

[16]Morrisette, E. L., and Goldberg, T. J., "Turbulent-Flow Separation Criteria for Overexpanded Supersonic Nozzles," NASA TP-1207, 1978.

[17]Chen, C. L., Chakravarthy, S. R., and Hung, C. M., "Numerical Investigation of Separated Nozzle Flows," *AIAA Journal*, Vol. 32, No. 9, 1994, pp. 1836–1843.

[18]Hamed, A., and Vogiatzis, C., "Overexpanded Two-Dimensional Convergent–Divergent Nozzle Performance, Effects of Three-Dimensional Flow Interactions," *Journal of Propulsion and Power*, Vol. 14, No. 2, 1998, pp. 234–240.

[19]Romine, G. L., "Nozzle Flow Separation," *AIAA Journal*, Vol. 36, No. 9, 1998, pp. 1618–1625.

[20]Hunter, C. A., "Experimental, Theoretical, and Computational Investigation of Separated Nozzle Flows," AIAA Paper 98-3107, July 1998.

[21]Frey, M., and Hagemann, G., "Restricted Shock Separation in Rocket Nozzles," *Journal of Propulsion and Power*, Vol. 16, No. 3, 2000, pp. 478–484.

[22]Murdock, J. W., and Welle, R. P., "Downstream Gas Effect on Nozzle Flow-Separation Location," *Journal of Propulsion and Power*, Vol. 17, No. 4, 2001, pp. 935–937.

[23]Beresh, S. J., Henfling, J. F., and Erven, R. J., "Surface Measurements of a Supersonic Jet in Subsonic Compressible Crossflow for the Validation of Computational Models," Sandia National Labs., Rept. SAND2002-1890, Albuquerque, NM, Oct. 2002.

[24]Shaw, R., "The Influence of Hole Dimensions on Static Pressure Measurements," *Journal of Fluid Mechanics*, Vol. 7, 1960, pp. 550–563.

[25]Guy, R. W., and Winebarger, R. M., "Effect of Orifice Size and Heat-Transfer Rate on Measured Static Pressures in a Low-Density Arc-Heated Wind Tunnel," NASA TN D-3829, Feb. 1967.

[26]Rainbird, W. J., "Errors in Measurement of Mean Static Pressure of a Moving Fluid due to Pressure Holes," *National Aeronautical Establishment Quarterly Bulletin*, 1967, No. 3, pp. 55–89.

[27]Moulden, T. H., Wu, J. M., Collins, F. G., and Ramon, H. J., "Experimental Study of Static Pressure Orifice Interference," Arnold Engineering Development Center, AEDC TR 77-57, June 1977.

[28]Flack, R. D., Jr., "Static Pressure Hole Errors in Transonic Flow with Pressure Gradients," *ISA Transactions*, Vol. 17, No. 4, 1978, pp. 89–95.

[29]Ducruet, C., and Dyment, A., "The Pressure-Hole Problem," *Journal of Fluid Mechanics*, Vol. 142, 1984, pp. 251–267.

[30]Ducruet, C., "A Method for Correcting Wall Pressure Measurements in Subsonic Compressible Flow," *Transactions of the ASME*, Vol. 113, No. 2, June 1991, pp. 256–260.

[31]Beresh, S. J., Henfling, J. F., and Erven, R. J., "Surface Measurements of a Supersonic Jet in Subsonic Compressible Crossflow," AIAA Paper 2001-2786, June 2001.

[32]Margason, R. J., "Fifty Years of Jet in Cross Flow Research," *Computational and Experimental Assessment of Jets in Cross Flow*, CP 534, AGARD, 1993, pp. 1.1–1.41.

[33]Cassel, L. A., Durando, N. A., Bullard, C. W., and Kelso, J. M., "Jet Interaction Control Effectiveness for Subsonic and Supersonic Flight," Rept. RD-TR-69-21, U. S. Army Missile Command, Redstone Arsenal, AL, Sept. 1969.

[34]Orth, R. C., and Funk, J. A., "An Experimental and Comparative Study of Jet Penetration in Supersonic Flow," *Journal of Spacecraft*, Vol. 4, No. 9, 1967, pp. 1236–1242.

[35]Kamotani, Y., and Greber, I., "Experiments on a Turbulent Jet in a Crossflow," *AIAA Journal*, Vol. 10, No. 11, 1972, pp. 1425–1429.

[36]Papamoschou, D., and Hubbard, D. G., "Visual Observations of Supersonic Transverse Jets," *Experiments in Fluids*, Vol. 14, No. 6, 1993, pp. 468–471.